Assembly of Optical-Scale Dumbbells into Dense Photonic Crystals

Jason D. Forster,[†,○] Jin-Gyu Park,[†,○] Manish Mittal,[‡,∥] Heeso Noh,[⊥] Carl F. Schreck,[§] Corey S. O'Hern,[†,§] Hui Cao,[⊥,§] Eric M. Furst,[‡,∥] and Eric R. Dufresne[†,§,¶,△,*]

[†]Department of Mechanical Engineering and Materials Science, Yale University, New Haven, Connecticut 06520, United States, [‡]Department of Chemical Engineering, University of Delaware, Newark, Delaware 19716, United States, [⊥]Department of Applied Physics, Yale University, New Haven, Connecticut 06520, United States, [§]Department of Physics, Yale University, New Haven, Connecticut 06520, United States, [∥]Center for Molecular and Engineering Thermodynamics, University of Delaware, Newark, Delaware 19716, United States, [¶]Department of Chemical and Environmental Engineering, Yale University, New Haven, Connecticut 06520, United States, and [△]Department of Cell Biology, Yale University, New Haven, Connecticut 06520, United States. [○]These authors contributed equally to this work.

Nanoscale colloidal particles with anisotropic interactions, or *colloidal molecules*, are expected to enable a wide range of materials with novel optical and mechanical properties.[1] However, robust and flexible processes for synthesizing large quantities of uniform nanoparticles with a variety of controlled shapes and interactions are only beginning to emerge.[2−6] With particles in hand, their self-assembly presents new challenges. While the self-assembly of spherical particles into periodic structures is relatively robust and well-characterized, the phase space describing the self-assembly of anisotropic particles is vast and has been only partially explored. It includes phases that are impossible for spherical particles to form, including gyroids,[7] simple cubic lattices,[8] and plastic crystals.[9] For dumbbells with excluded-volume interactions, numerical experiments suggest that aspect ratio plays a key role in determining equilibrium phase behavior. At small aspect ratios and high volume fractions, dumbbells form plastic crystals, which possess long-range translational order of particle centers without long-range correlations of particle orientations. Higher aspect ratio dumbbells form crystals with ordered particle orientations.[9,10] Dumbbell-based crystals have been predicted to have interesting optical properties. Calculations have shown that complete photonic band gaps should exist for crystals composed of dumbbell particles with asymmetric lobes.[11]

While their potential is great, the additional degrees of freedom of anisotropic particles that enable the formation of new structures also complicate and frustrate the kinetic pathways of self-assembly. Previous studies on self-assembly of ellipsoids and dumbbells in the absence of external fields

ABSTRACT We describe the self-assembly of nonspherical particles into crystals with novel structure and optical properties combining a partial photonic band gap with birefringence that can be modulated by an external field or quenched by solvent evaporation. Specifically, we study symmetric optical-scale polymer dumbbells with an aspect ratio of 1.58. Hard particles with this geometry have been predicted to crystallize in equilibrium at high concentrations. However, unlike spherical particles, which readily crystallize in the bulk, previous experiments have shown that these dumbbells crystallize only under strong confinement. Here, we demonstrate the use of an external electric field to align and assemble the dumbbells to make a birefringent suspension with structural color. When the electric field is turned off, the dumbbells rapidly lose their orientational order and the color and birefringence quickly go away. In this way, dumbbells combine the structural color of photonic crystals with the field addressability of liquid crystals. In addition, we find that if the solvent is removed in the presence of an electric field, the particles self-assemble into a novel, dense crystalline packing hundreds of particles thick. Analysis of the crystal structure indicates that the dumbbells have a packing fraction of 0.7862, higher than the densest known packings of spheres and ellipsoids. We perform numerical experiments to more generally demonstrate the importance of controlling the orientation of anisotropic particles during a concentration quench to achieve long-range order.

have not succeeded in making large-scale periodic structures.[3,12] To surmount this challenge, several strategies have been proposed. Originally, mechanical forces were successfully applied to deform crystals of spherical particles into crystals of ellipsoids.[13,14] Alternatively, external electromagnetic fields can also align particles and facilitate crystallization. Magnetic fields have been very successful in aligning ellipsoids, resulting in large-scale crystals.[15,16] However, manipulation with magnetic fields requires materials with a high magnetic susceptibility, which significantly reduces the scope of available materials. On the other hand, ac electric fields offer many advantages. First, electric fields generically

couple to dielectric and metallic materials. Second, electric fields can be readily modulated on-chip to control suspension structure dynamically. Finally, in addition to the magnitude and direction of the field, interactions can depend strongly on the frequency of the applied field. For example, the preferred orientation of ellipsoidal particles relative to an ac electric field can depend on the frequency.[17] Alternating current electric fields have been used to align titania ellipsoids[17] and to create crystals of micrometer-scale dumbbells.[18]

Here, we describe the formation of large crystals of optical scale dumbbells by electric field assisted self-assembly and characterize their structure and photonic properties. We demonstrate that dumbbell crystals display both the structural color associated with photonic crystals and the birefringence and field-addressability of liquid crystals. Furthermore, we perform numerical simulations of self-assembly that highlight the critical importance of external fields in crystallizing even simple anisotropic particles.

RESULTS AND DISCUSSION

We synthesize large quantities of monodisperse polymer dumbbells at optical length scales using a recently described process.[3] Briefly, we start with a suspension of monodisperse polystyrene spheres and swell them with a mixture of styrene and trimethoxysilylpropylacrylate. Upon polymerization, these particles develop a spherical core-shell structure and form dumbbells after another swelling and polymerization step. The relative sizes of the two lobes can be controlled by varying the amount of monomer used in each step.[19] The particles we use here have two lobes of the same size, with a diameter of 267 ± 5 nm and an overall length of 422 ± 7 nm, giving them a length-to-diameter ratio, α, of 1.58.

While these dumbbells readily crystallize in confined films,[3] they resist crystallization in the bulk. As the film thickness increases, dumbbells form ordered monolayers laying down, ordered monolayers standing up, as shown in Figure 1a, and three variations of ordered bilayers (down/down, down/up, and up/up).[3] However, when these dumbbells are dried into thicker films, they pack randomly, as shown in Figure 1b. These observations are at odds with numerical simulations
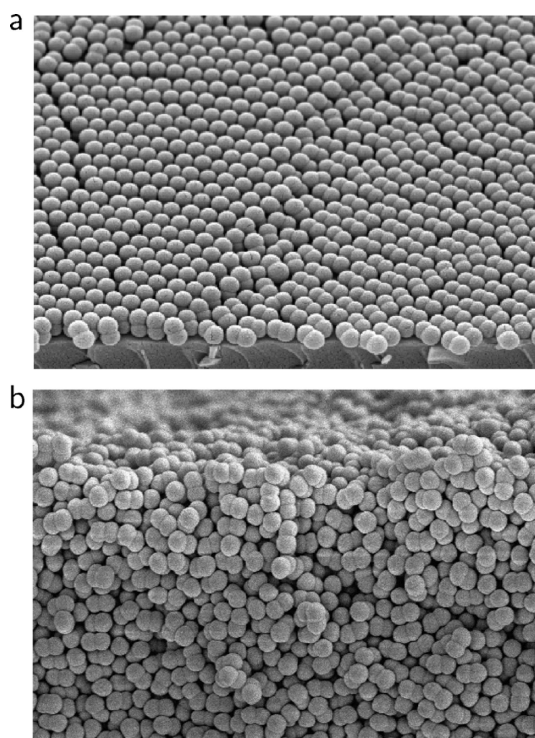

Figure 1. Dumbbells crystallize in confinement, but not in the bulk. (a) SEM image of dry dumbbells cast into thin films by vertical deposition. Dumbbells form ordered mono- and bilayers.[3] (b) SEM image of dumbbells cast into an amorphous thick film. The fields of view in (a) and (b) are 7.6 μm across.
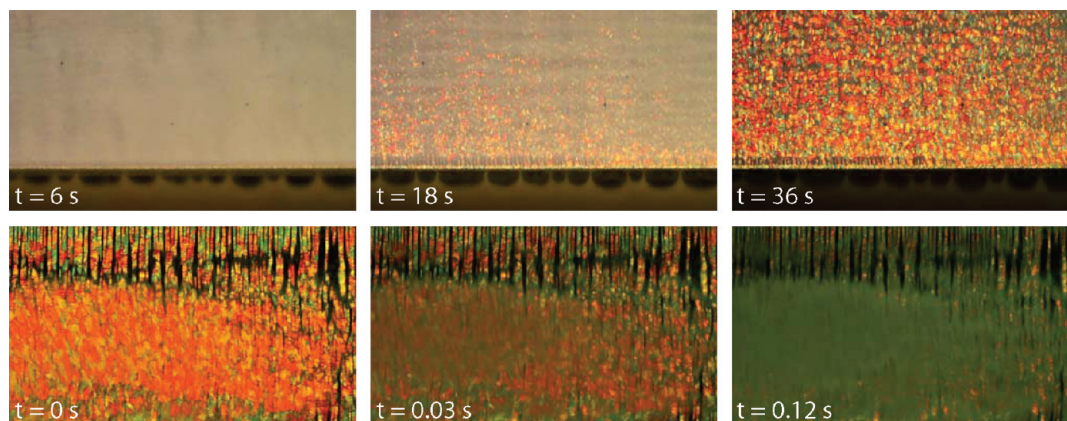

Figure 2. Aqueous suspensions of dumbbells display reversible crystallization in ac electric fields. Aqueous suspension of dumbbells at volume fraction $\phi = 0.13$. Top row: Snapshots showing the onset of crystallization in an aqueous suspension of dumbbells in an ac electric field. The dark stripe across the bottom of the frame is a gold electrode. The sample is imaged through crossed polarizers. Bottom row: Snapshots showing the rapid loss of structural color and birefringence when the electric field is turned off. The whole process can be seen in Supplementary Movie 1. The field of view in each image is 1.4 mm across.
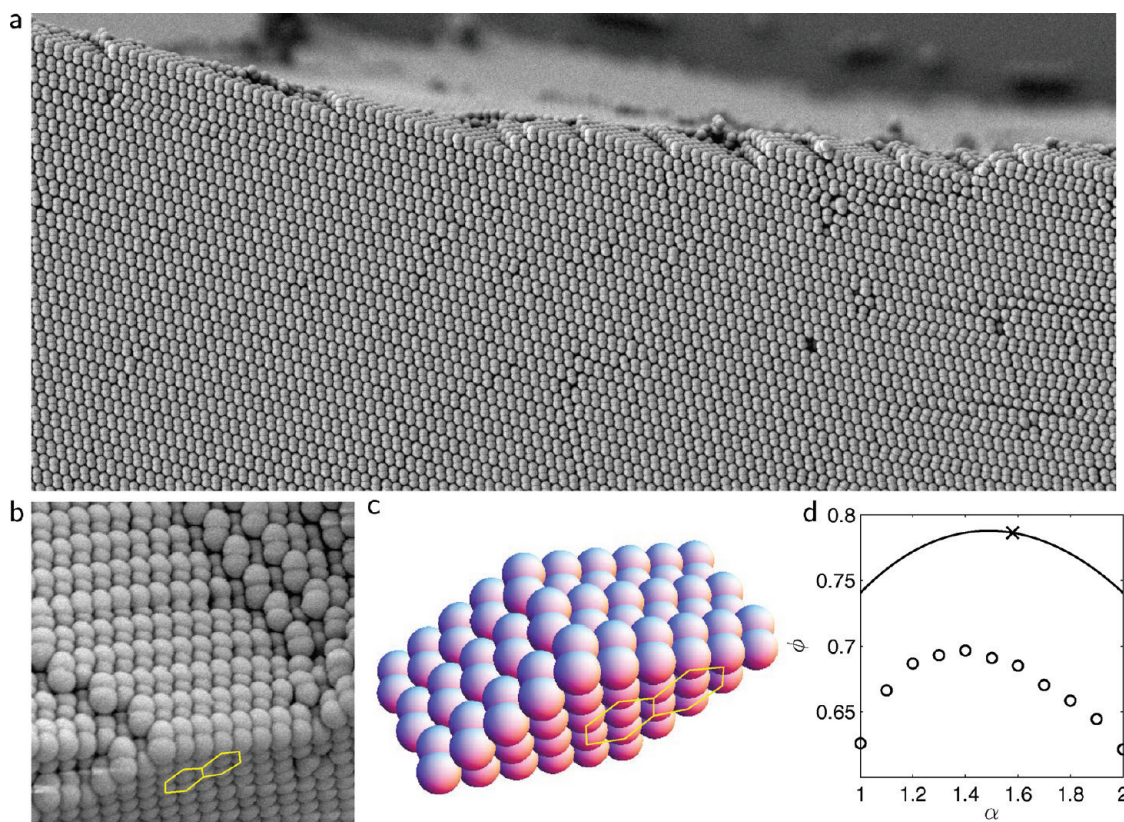
Figure 3. Crystal structure of suspension dried in an ac electric field. (a) SEM image of crystal formed by drying a suspension of dumbbells in the presence of an electric field. In this image, the electric field orientation is approximately vertical and the direction of flow due to drying is from right to left. The field of view is 27 μm across. **(b)** SEM image highlighting crystal structure. Two adjoining hexagons formed by the dumbbell lobes are highlighted by the yellow hexagons. The field of view is 3.6 μm across. **(c)** Model of the crystal structure suggested by SEM images. Two adjoining hexagons are highlighted and correspond to the highlighted facet in (b). **(d)** Packing fraction *versus* aspect ratio for crystalline structures (line) and random, jammed packings (circles) generated from numerical simulations described in the Methods section. The packing fraction for the aspect ratio 1.58 dumbbells in a crystalline structure is $\phi = 0.7862$ ($\times$).

predicting the equilibrium phase diagram of hard dumbbells, which suggests that these particles should form structures with long-range order in thermodynamic equilibrium at these volume fractions.[9]

To adopt a crystalline packing, dumbbells not only have to arrange themselves on a periodic lattice but also have to orient themselves in a specific direction. In order to facilitate crystallization, we bias the particle orientations with an external electric field.[17,20,18] The anisotropic polarizability of dumbbells causes them to align themselves with the direction of the electric field. The applied electric field also introduces long-range interactions between particles that tend to locally concentrate the suspension.[21−24] In Figure 2, we demonstrate the capability to control the structure of dumbbell suspensions with an external electric field. With no applied electric field, the suspension is strongly scattering with no structural color or birefringence. Initially, the sample is gray when viewed under crossed polarizers because the random orientations and positions of the dumbbells act to mix the polarization of light propagating through the sample. We then apply an ac electric field (f = 50 kHz, E = 1040 V/cm)

with coplanar gold electrodes separated by a 0.85 mm gap in a 20 μm thick glass sample chamber; a schematic of the chamber is shown in Supplementary Figure 1. About six seconds after the field is turned on we see a wave of birefringence originating from the electrodes, where the electric field strength is highest. Within 36 s, there is strong birefringence and structural color visible across the sample. The patchwork of structural color across the sample points to polycrystalline domains on the order of 7 μm in width. The crystallites can be further compacted by a step change in the frequency of the applied electric field (from 50 to 10 kHz), as shown in Supplementary Movie 2, which changes the form of the interparticle dipole interaction.[24] While we have not yet been able to characterize the structure of these crystals, we expect that they adopt similar structures to those that have been recently described for micrometer-scale dumbbells in external electric fields.[18] When the electric field is turned off, structural color and birefringence rapidly disappear. Field-switchable photonic crystals have previously been demonstrated with spherical particles,[25] but suspensions of dumbbells may offer
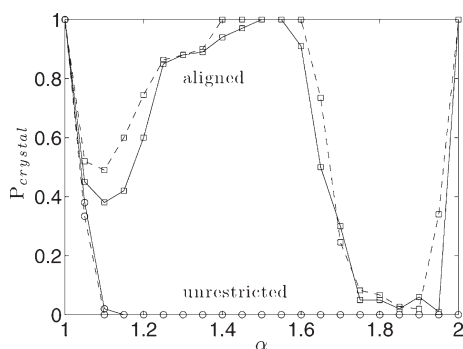
Figure 4. Simulations demonstrate crystal formation depends strongly upon control of dumbbell orientation. Probability of crystallization for a system of dumbbells as a function of aspect ratio. Systems with aligned dumbbells (squares) have significant probabilities of crystallization for most aspect ratios. Systems with unrestricted dumbbell orientations (circles) have near zero probabilities of crystallization for aspect ratios greater than 1.1. Each point is the result of 100 independent simulations. The two line types represent simulations performed with different quench rates; the dashed line has a quench rate that is 1000 times lower than the solid line.

more flexibility—due to their ability to adopt different crystalline structures and greater speed—by allowing dramatic changes to optical properties through mere particle reorientation and not complete reorganization of the underlying suspension structure.

To assemble stable crystalline packings, we dry dumbbell suspensions in the presence of an electric field. The crystal seen in Figure 3a is approximately one hundred particles thick (additional images can be seen in Supplementary Figures 3−6) and is the result of the application of an ac electric field (f = 50 kHz, E = 1040 V/cm) during the unidirectional drying of an aqueous suspension of dumbbells with initial volume fraction, ϕ, of 0.13.[17]

The crystal structure formed by dumbbells is more complicated than the cubic structures formed by spherical particles. SEM images of the dumbbell crystals reveal a number of features that allow us to identify the structure. At the bottom of Figure 3b one can see lobes of the dumbbells in hexagonally packed layers, highlighted by yellow hexagons, with the major axis of the dumbbells tilted relative to the normal of these planes. Successive layers pack such that the hexagonally packed bottom lobes of a new layer fit into the hexagonally packed top lobes of the previous layer.

This layering scheme allows for successive layers to fit snugly together for any particle tilt, as long as the top and bottom lobes of each particle can remain in contact with the top and bottom lobes of its six nearest neighbors. For ordered close-packed spheres, there are three possible translational alignments of one hexagonally packed layer with respect to the next, which specify the familiar fcc, hcp, and rhcp packings. Dumbbells have an additional 3-fold orientational degeneracy, due to the tilting of the particles within each layer.

However, in an applied electric field, the dumbbells tend to maintain a constant orientation from plane to plane, as shown in Figure 3a,b. A schematic of this packing is shown in Figure 3c. During drying, capillary forces tend to drive suspended particles toward their densest packing. To our knowledge, this packing, which was found to be an equilibrium structure of hard dumbbells,[9] is the densest packing of symmetric dumbbells. In numerical simulations, we have verified that this packing is mechanically stable and at least a local maximum in the packing density, as described in Supplementary Figure 7.

These structures have very high packing fractions. For the dumbbells used in our experiments, the packing fraction is ϕ = 0.7862. This packing fraction is significantly higher than both the densest crystalline sphere packing, ϕ_{sphere}^{fcc} = 0.7405, and the densest known crystalline packing of ellipsoids, $\phi_{ellipsoid}$ = 0.7707.[26] Figure 3d shows the anticipated packing fraction of dumbbells in this crystal structure as a function of aspect ratio, $\phi = [((3 - \alpha)\alpha^2)/(2 + (\alpha - 1)(6 - 2(\alpha - 1)^2)^{1/2})]\phi_{sphere}^{fcc}$. The aspect ratio that gives the highest packing fraction is 1.5, with ϕ = 0.7877. The dumbbell tilt angle for the crystal structure depends on the aspect ratio, as shown in Supplementary Figure 8. For aspect ratios 1.5 and 1.58, the tilt angles for the crystal structure are 16.8° and 19.5°, respectively.

Our experiments suggest that restricting the orientation of the dumbbells is critical to achieving crystallization; numerical simulations of the jamming of dumbbells under compression yield similar findings. We perform numerical simulations of mechanically stable dumbbell packings by successively compressing and decompressing the system and relaxing the energy until all forces are balanced and interparticle overlaps are vanishingly small.[27] The probability of the system crystallizing as a function of aspect ratio α for slow thermal quench rates is plotted in Figure 4. In the absence of an external field that favors alignment, systems of dumbbells with α higher than 1.1 have essentially zero probability of crystallizing at the quench rates explored here. By contrast, restricting particle orientations dramatically increases the probability of crystallization. In that case, the probability of crystallization is highest for aspect ratios between 1.2 and 1.6. Previous Monte Carlo simulations predict that the crystalline phase we observe should be thermodynamically stable for α greater than 1.3 even in the absence of an external field.[10] However, in our simulations in the absence of the field, the particles form amorphous mechanically stable packings at densities that are systematically lower than their crystalline counterparts, as plotted in Figure 3d, and also lower than random jammed packings of oblate ellipsoids.[26,28] We find that lowering the quench rate used in our simulations by a factor of 1000 does not have a significant effect on the probability of
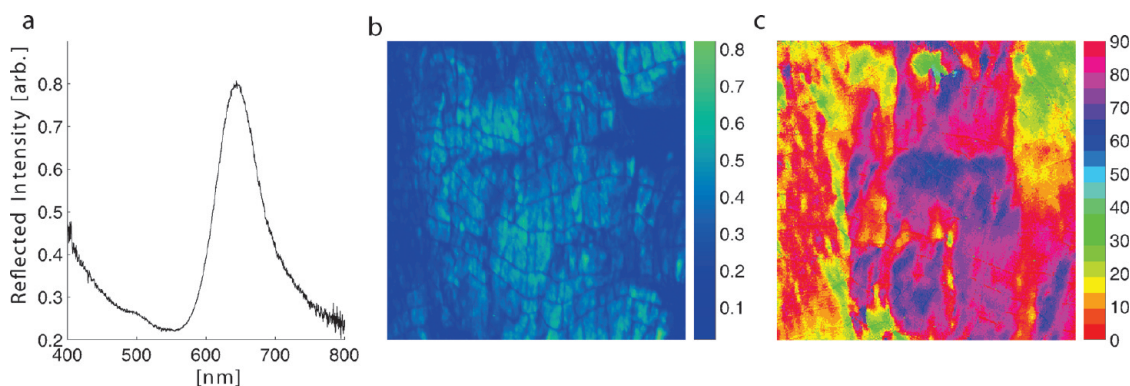
Figure 5. Dumbbell crystals have a partial photonic band gap and are birefringent. (a) Normal incidence reflection spectrum from a 70 μm × 70 μm area of a dumbbell crystal. The peak at 644 nm is close to the predicted photonic band gap position for the probed direction (band diagram in Supplementary Figure 9). Images of (b) the depth and (c) phase of the modulation (in degrees) of transmitted light with the rotation of crossed polarizers measured at a wavelength of 650 nm inside the band gap. The electric field direction relative to this image is vertical. The field of view in both (b) and (c) is 600 μm across.

crystallization for either the aligned or unrestricted dumbbells, as seen in Figure 4.

These dumbbell crystals have partial photonic band gaps. Figure 5a shows a normal incidence reflection spectrum of a 70 μm × 70 μm area of a dumbbell crystal. We see a strong peak in the reflectance at 644 nm with a full width at half-maximum (fwhm) of 72 nm. Using our model of the crystal structure, we calculate the photonic band structure. These calculations show partial band gaps in certain crystal directions, as described in Supplementary Figure 9. In the direction optical reflection was probed (Figure 5a), the predicted photonic band gap is centered at 660 nm with a fwhm of 30 nm. The center wavelength matches well that of the reflection peak in Figure 5a, but the width is significantly smaller. We believe the presence of multiple domains with different crystal orientations, as seen in the SEM images, leads to a spectral broadening of the reflectance peak.

In addition to having a photonic band gap, these dumbbell crystals are birefringent. To visualize the birefringence, we image the crystals through crossed polarizers using wavelengths inside and outside the band gap (650 and 534 nm). For both wavelengths, we observe a sinusoidal modulation of the transmitted intensity with the relative angle of the sample and crossed polarizers, as shown in Supplementary Movies 3 (650 nm) and 4 (534 nm). The depth and phase of the modulation vary from location to location within the sample, as shown in Figure 5b,c and Supplementary Figure 10. Depolarization of transmitted light inside the band gap is expected from the previous studies of colloidal crystals by Monovoukas *et al.* due to the polarization-dependent efficiency of Bragg diffraction from the crystal structure.[29] This study also found that crystals of spheres showed no birefringence outside the photonic band gap. In contrast, we do observe strong birefringence outside of the band gap, which we believe originates from the anisotropic shape of individual dumbbell particles.

Anisotropic colloidal particles can self-assemble into crystalline structures with long-range order in the presence of an external field. Crystals of anisotropic particles have novel optical properties that combine photonic band gaps with birefringence. Furthermore, anisotropic particles could improve the speed and functionality of field-switchable photonic crystals.

METHODS

SEM Imaging and Dumbbell Sizes. The SEM images in Figure 1, and Supplementary Figure 4 were obtained with a Philips XL-30 ESEM with an acceleration voltage of 10 kV. The SEM image in Figure 3b was recorded with a Hitachi SU-70 SEM with an acceleration voltage of 10 kV. The SEM images in Figure 3a, and Supplementary Figures 4, 5, and 6 were recorded with a JEOL-7400f SEM with an acceleration voltage of 2 kV. Samples were coated with a thin layer of gold prior to imaging. Dumbbell sizes were measured by analyzing SEM images of 30 isolated dumbbells.

Movies of Aqueous Suspensions of Dumbbells in an ac Electric Field. Aqueous suspensions of dumbbells with $\phi = 0.13$ were placed in an ac electric field, generated by amplifying a sine wave generated using a function generator. The sample cell is approximately 20 μm thick, and the spacing between the electrodes is 0.85 mm. The electric field frequency is $f = 50$ kHz, and field strength $E = 1040$ V/cm. The sample cell is placed between crossed polarizers, which are at an angle of approximately 45° to the field direction. The movies are recorded on an inverted Axiovert 200 Zeiss microscope using a digital SLR camera (Canon-EOS Digital Rebel T1i).

Simulations of Dumbbell Packing. We performed extensive numerical simulations of soft dumbbell particles composed of two rigidly constrained spheres. The interactions between dumbbell particles arise from purely repulsive, pairwise linear spring forces that act centrally between the centers of the spheres that comprise two different dumbbells. We generated mechanically stable dumbbell packings via isotropic compression—by successively compressing and decompressing the system and relaxing the energy until all forces and torques were balanced

and interparticle overlaps were vanishingly small using the algorithm described in detail in ref 27.

To create the amorphous mechanically stable dumbbell packings described in Figure 3d, we initialized the system in a dilute state at packing fraction $\phi_0 = 0.2$ with random dumbbell positions and orientations inside a unit cube. We chose the increment in packing fraction as $\Delta\phi \leq 10^{-4}$ and the final potential energy $V/\varepsilon N$ of the packing to be in the range $10^{-16} < V/\varepsilon N < 2 \times 10^{-16}$, where ε is the characteristic energy scale of the repulsive interaction and $N = 512$ is the number of dumbbells.

We also performed simulations to compare the probability to form a crystalline structure in the presence and absence of a strong aligning field as shown in Figure 4 in systems ranging from $N = 27$ to 125 particles. We thermally quenched equilibrated fluid systems at $\phi_0 = \phi_{xstal} - 0.2$ and $k_bT/\varepsilon = 10^{-3}$ by linearly decreasing the temperature to $T = 0$ over a wide range of thermal quench rates $10^{-2} > rk_bT\tau/\varepsilon > 10^{-9}$ to generate the initial configurations, where τ is a typical collision time between dumbbells. In Figure 4, we show results for $rk_bT\tau/\varepsilon = 10^{-6}$ and $rk_bT\tau/\varepsilon = 10^{-9}$ since these rates yield fcc packings for spheres. We then used the isotropic compression protocol described above with initial configurations from the thermal quenches to generate dumbbell packings. To simulate a strong aligning field, the orientations were initially chosen to be consistent with the crystalline packing at each aspect ratio and then prevented from evolving during the thermal quench and isotropic compression packing algorithm. The fraction of crystalline packings, P_{xtal}, was determined as the ratio of the number of packings with $|\phi_{xstal} - \phi_J| < 10^{-6}$ to the total number of trials.

Optical Spectra. The reflection spectrum in Figure 5a was measured with a Nikon Optiphot 66 microscope in epi-scopic mode. We used a $40\times$ objective lens for illumination and collection of reflected light. We used a field stop to reduce the size of the illumination and collection area to 70 μm $\times$ 70 μm. The reflected light was transferred to an Ocean optics HR2000+ spectrometer through an optical fiber. The reflection spectrum was normalized to the spectrum recorded from an Ocean Optics reflection standard.

The images of transmitted intensity during the rotation of crossed polarizers in Figure 5b,c and Supplementary Figure 10 were recorded on a Nikon TE-2000 inverted optical microscope with a Photron FASTCAM 1024 PCI camera. The halogen bright field lamp on the microscope was used for illumination, and colored filters were used to select wavelengths inside and outside the photonic band gap.

Supporting Information Available: Ten figures and four movies are available. This material is available free of charge *via* the Internet at http://pubs.acs.org.

REFERENCES AND NOTES

1. Glotzer, S. C.; Solomon, M. J. Anisotropy of Building Blocks and Their Assembly Into Complex Structures. *Nat. Mater.* **2007**, *6*, 380–382.
2. Duguet, E.; Desert, A.; Perro, A.; Ravaine, S. Design and Elaboration of Colloidal Molecules: an Overview. *Chem. Soc. Rev.* **2011**, *40*, 941–960.
3. Park, J. G.; Forster, J. D.; Dufresne, E. R. High-Yield Synthesis of Monodisperse Dumbbell-Shaped Polymer Nanoparticles. *J. Am. Chem. Soc.* **2010**, *132*, 5960–5961.
4. Kuijk, A.; van Blaaderen, A.; Imhof, A. Synthesis of Monodisperse, Rodlike Silica Colloids with Tunable Aspect Ratio. *J. Am. Chem. Soc.* **2011**, *133*, 2346–2349.
5. Jiang, S.; Schultz, M. J.; Chen, Q.; Moore, J. S.; Granick, S. Solvent-Free Synthesis of Janus Colloidal Particles. *Langmuir* **2008**, *24*, 10073–10077.
6. Perro, A.; Reculusa, S.; Ravaine, S.; Bourgeat-Lami, E.; Duguet, E. Design and Synthesis of Janus Micro- and Nanoparticles. *J. Mater. Chem.* **2005**, *15*, 3745–3760.
7. Ellison, L. J.; Michel, D. J.; Barmes, F.; Cleaver, D. J. Entropy-Driven Formation of the Gyroid Cubic Phase. *Phys. Rev. Lett.* **2006**, *97*, 237801.
8. Rossi, L.; Sacanna, S.; Irvine, W. T. M.; Chaikin, P. M.; J., P. D.; Philipse, A. P. Cubic Crystals from Cubic Colloids. *Soft Matter* **2011**, *7*, 4139–4142.
9. Vega, C.; Paras, E. P. A.; Monson, P. A. Solid-Fluid Equilibria for Hard Dumbbells via Monte Carlo Simulation. *J. Chem. Phys.* **1992**, *96*, 9060–9072.
10. Vega, C.; Paras, E. P. A.; Monson, P. A. On the Stability of the Plastic Crystal Phase of Hard Dumbbell Solids. *J. Chem. Phys.* **1992**, *97*, 8543–8548.
11. Hosein, I. D.; Ghebrebrhan, M.; Joannopoulos, J. D.; Liddell, C. M. Dimer Shape Anisotropy: A Nonspherical Colloidal Approach to Omnidirectonal Photonic Band Gaps. *Langmuir* **2010**, *26*, 2151–2159.
12. Hosein, I. D.; Lee, S. H.; Liddell, C. M. Dimer-Based Three-Dimensional Photonic Crystals. *Adv. Funct. Mater.* **2010**, *20*, 3085–3091.
13. Lu, Y.; Yin, Y.; Li, Z. Y.; Xia, Y. Colloidal Crystals Made of Polystyrene Spheroids: Fabrication and Structural/Optical Characterization. *Langmuir* **2002**, *18*, 7722–7727.
14. Lele, P. P.; Furst, E. M. Assemble-and-Stretch Method for Creating Two- and Three-Dimensional Structures of Anisotropic Particles. *Langmuir* **2009**, *25*, 8875–8878.
15. Ding, T.; Song, K.; Clays, K.; Tung, C. H. Fabrication of 3D Photonic Crystals of Ellipsoids: Convective Self-Assembly in Magnetic Field. *Adv. Mater.* **2009**, *21*, 1936–1940.
16. Ding, T.; Song, K.; Clays, K.; Tung, C. H. Controlled Directionality of Ellipsoids in Monolayer and Multilayer Colloidal Crystals. *Langmuir* **2010**, *26*, 11544–11549.
17. Mittal, M.; Furst, E. M. Electric Field-Directed Convective Assembly of Ellipsoidal Colloidal Particles to Create Optically and Mechanically Anisotropic Thin Films. *Adv. Funct. Mater.* **2009**, *19*, 3271–3278.
18. Demirors, A. F.; Johnson, P. M.; van Kats, C. M.; van Blaaderen, A.; Imhof, A. Directed Self-Assembly of Colloidal Dumbbells with an Electric Field. *Langmuir* **2010**, *26*, 14466–14471.
19. Sheu, H. R.; El-Aasser, M. S.; Vanderhoff, J. W. Phase Separation in Polystyrene Latex Interpenetrating Polymer Networks. *J. Polym. Sci., Polym. Chem.* **1990**, *28*, 629–651.
20. Grzelczak, M.; Vermant, J.; Furst, E. M.; Liz-Marzan, L. M. Directed Self-Assembly of Nanoparticles. *ACS Nano* **2010**, *4*, 3591–3605.
21. Fraden, S.; Hurd, A. J.; Meyer, R. B. Electric-Field-Induced Association of Colloidal Particles. *Phys. Rev. Lett.* **1989**, *63*, 2373–2376.
22. Yethiraj, A.; van Blaaderen, A. A Colloidal Model System with an Interaction Tunable from Hard Sphere to Soft and Dipolar. *Nature* **2003**, *421*, 513–517.
23. Gong, T.; Wu, D. T.; Marr, D. W. M. Electric-Field Reversible Three-Dimensional Colloidal Crystals. *Langmuir* **2003**, *19*, 5967–5970.
24. Mittal, M.; Lele, P. P.; Kaler, E. W.; Furst, E. M. Polarization and Interactions of Colloidal Particles in AC Electric Fields. *J. Chem. Phys.* **2008**, *129*, 064513.
25. Lumsdon, S. O.; Kaler, E. W.; Williams, J. P.; Velev, O. D. Dielectrophoretic Assembly of Oriented and Switchable Two-Dimensional Photonic Crystals. *Appl. Phys. Lett.* **2003**, *82*, 949–951.
26. Donev, A.; Stillinger, F. H.; Chaikin, P. M.; Torquato, S. Unusually Dense Crystal Packings of Ellipsoids. *Phys. Rev. Lett.* **2004**, *92*, 255506.
27. Gao, G. J.; Blawzdziewicz, J.; O'Hern, C. S. Frequency Distribution of Mechanically Stable Disk Packings. *Phys. Rev. E* **2006**, *74*, 061304.
28. Donev, A.; Cisse, I.; Sachs, D.; Variano, E. A.; Stillinger, F. H.; Connelly, R.; Torquato, S.; Chaikin, P. M. Improving the Density of Jammed Disordered Packings Using Ellipsoids. *Science* **2004**, *303*, 990–993.
29. Monovoukas, Y.; Fuller, G. G.; Gast, A. P. Optical Anisotropy in Colloidal Crystals. *J. Chem. Phys.* **1990**, *93*, 8294–8299.